Fast trailed and bound vorticity modeling of swept wind turbine blades

Li, Ang; Pirrung, Georg; Madsen, Helge Aa; Gaunaa, Mac; Zahle, Frederik

Published in:
Journal of Physics: Conference Series

Link to article, DOI:
10.1088/1742-6596/1037/6/062012

Publication date:
2018

Document Version
Publisher's PDF, also known as Version of record

Fast trailed and bound vorticity modeling of swept wind turbine blades

IOP Conf. Series: Journal of Physics: Conf. Series **1037** (2018) 062012 doi:10.1088/1742-6596/1037/6/062012

Fast trailed and bound vorticity modeling of swept wind turbine blades

Ang Li, Georg Pirrung, Helge Aa. Madsen, Mac Gaunaa and Frederik Zahle

Wind Energy Department, Technical University of Denmark, Frederiksborgvej 399, DK-4000 Roskilde, Denmark

E-mail: angl@dtu.dk

Abstract. Passive load alleviation can be achieved through geometric bend-twist coupling, for example, by sweeping the blade backwards. The influence of the blade sweep on the trailing vorticity and bound vorticity is not modelled in the current fast aeroelastic wind turbine codes suitable for certification. A near wake trailed vorticity model which was coupled with a blade element momentum theory based aerodynamic model has been modified to take into account the blade sweep. The extended model is compared with the original near wake model, a blade element momentum (BEM) model and full rotor computational fluid dynamics (CFD) results for the modified IEA 10MW reference wind turbines. The steady-state loadings calculated from the extended model are in better agreements with CFD compared to the original model and the BEM for four different swept blades. It is also shown that the influence of the blade sweep on normal loading is not correctly modelled by BEM and this error will be inherited to the near wake model results. Thus, further modification to BEM will likely improve the predicted normal loading for swept blades, even if no near wake model is used.

1. Introduction

The aerodynamic models that are typically used in the state-of-the-art aeroelastic wind turbine codes are based on the blade element momentum (BEM) theory. These BEM models are usually extended by a tip loss correction and dynamic inflow models to take into account the wake inertia. The near wake model (NWM) was originally formulated by Beddoes [1]. In order to account for some of the shortcomings in the BEM type modelling (e.g. strip theory which means no coupling of aerodynamics along the blade) the near wake model was considered for wind turbine applications by Madsen and Rasmussen [2]. It was further extended for aeroelastic simulations as part of a coupled near and far wake model by Pirrung [3, 4]. In this model, the NWM and a far wake BEM are coupled through a coupling factor [5] to match the total thrust calculated from a reference BEM.

For modern wind turbines, backwards-swept blades are favourable because of the passive load reduction through structural bend-twist coupling. For the swept blades, the locations where the vorticities start being trailed are different from that of the straight blade causing a modified induction along the blade. In addition, the non-straight lifting line due to the blade sweep will also introduce additional induced velocity. These effects will then influence the load distribution of the whole blade especially towards the tip where strong vortices are trailed and where the sweep is usually applied. Because tip loss corrections have been developed for straight blades,

the influences of blade sweep on trailing vorticity and curved lifting line are not modelled in any state-of-the-art BEM based aerodynamic models.

In this work, the trailed vorticity model extended in [3, 4] and implemented in the aeroelastic code HAWC2 [6] is further modified to model the trailed vorticity as well as the curved lifting line of swept blades. The results from this modified model are validated against the results calculated using the CFD solver Ellipsys3D [7]. The wind turbine blades that are used for the validation are modified based on IEA-10.0-198 10MW reference wind turbine (RWT) [8] which has a rotor diameter of 198m.

2. Near wake model description

The NWM was originally developed by Beddoes for use in helicopter aerodynamics. The original model was developed assuming in-plane trailed vorticity. The model was extended to model both helical vortex arcs and standstill conditions by Pirrung [3, 4]. The induced velocity is approximated with two exponential functions which made it possible for the indicial function algorithm to be used. The computational effort will then be much less than numerical integration of the Biot-Savart law.

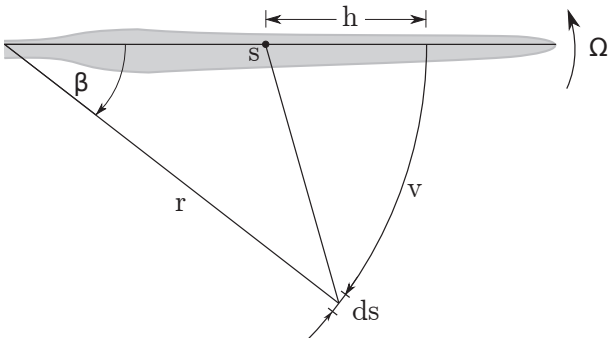

Figure 1. Sketch of the geometry of the straight blade in the near wake. The variable of r is defined to be the radius of the vortex trailing point and the variable of h is the difference of the radius of the vortex trailing point v and section point s. If $h > 0$, the section point is further inboard compared to the vortex trailing point and if $h < 0$, the section point is further outboard. The figure is from Pirrung et al., [3].

A sketch of the geometry of the near wake is shown in Figure 1. The induction W at blade section point s at time step i is the summation of the induced velocities due to all the vortex arcs trailed from the trailing point v.

$$W_s^i = \sum_{v=1}^{N_v} W_{s,v}^i = \sum_{v=1}^{N_v} (X_{w,s,v}^i + Y_{w,s,v}^i) \tag{1}$$

where $X_{w,s,v}^i$ and $Y_{w,s,v}^i$ are the fast and slow component of the induced velocity $W_{s,v}^i$, and are approximated with exponential functions.

The induced velocity in a new time step is then calculated with indicial functions. The trailed vorticity strength is $\Delta\Gamma$ and is dependent on the gradient of the radial distribution of the unsteady bound circulation. Its quasi-steady value is calculated with Equation 2, and the unsteady value is approximated by the three term indicial function [9].

$$\Gamma_{QS} = \frac{1}{2} v_r c C_L \tag{2}$$

The variable of $D_{x,s,v}$ and $D_{y,s,v}$ are the fast and slow components of the normalized induced velocity at section s due to the trailed vortex v with unit strength which just trailed from the blade. The induction due to the vortex arc trailed in this time step is added to the induced velocity of the previous time step. This induced velocity from the previous time step is multiplied by exponential decay factors. These factors are dependent on the geometric parameter Φ, which depends on the positions of vortex trailing point, section point and the trailed vortex helix angle φ [3].

$$X^i_{w,s,v} = X^{i-1}_{w,s,v} e^{-\Delta\beta/\Phi_{s,v}} + D_{x,s,v}\Delta\Gamma(1 - e^{-\Delta\beta/\Phi_{s,v}}) \tag{3}$$

$$Y^i_{w,s,v} = Y^{i-1}_{w,s,v} e^{-4\Delta\beta/\Phi_{s,v}} + D_{y,s,v}\Delta\Gamma(1 - e^{-4\Delta\beta/\Phi_{s,v}}) \tag{4}$$

Finally, the axial and tangential components of the induced velocity can be calculated with the trigonometric projections with φ, which is proposed by Wang and Coton [10].

3. Model extension

In order to model the geometry of the swept blade, an additional variable ψ is introduced. It is defined to be the difference of the azimuthal location of the vortex trailing point v and the section point s. The definition of the variable r and h is in consistency with the original definition for the straight blade. A sketch of the near wake geometry of a backward swept blade is shown in Figure 2. To be noted that the definition of β is identical to [3], which is the azimuthal angle of the vorticity has trailed in the rotor plane.

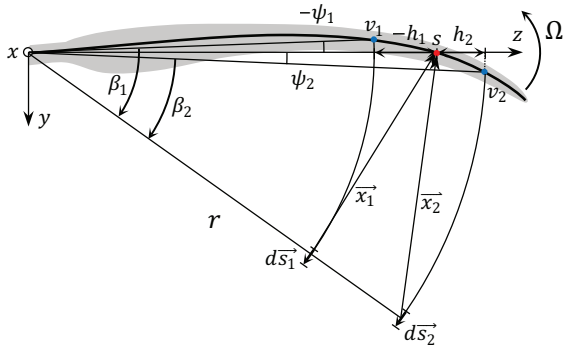

Figure 2. Sketch of the geometry of the swept blade in the near wake. The vortex trailed from point v_1 is in-board and ahead of the section s corresponds to $\psi_1 < 0$, and the vortex trailed from point v_2 is out-board and behind compared to the section s corresponds to $\psi_2 > 0$.

The induction due to trailed vorticity behind the swept blades and the curved lifting line are computed separately, as explained in Sections 3.1 and 3.2.

3.1. Trailed vorticity

The modification to the NWM to model the trailed vorticity of the swept blade is introduced as follows. When calculating the induced velocity at section s, the corresponding coordinate system is defined so that the x-axis is in the upwind direction, the y-axis is in the tangential direction of this section pointing towards trailed vorticity and z-axis is pointing from the root to the section point s. The coordinate system is shown in Figure 2. To be noted that for different section points, the coordinate systems will be rotated around the x-axis according to the blade sweep.

3.1.1. Analytical equations In the following, the analytical trailing function of the swept blade is derived with similar method as Pirrung [3]. The vector $\vec{x}$ is pointing from the location of the trailed vortex filament to the section point s, and $\vec{ds}$ is pointing away from the blade. The aforementioned two variables are expressed as function of r, h, β and ψ as follows:

$$\vec{x} = \begin{pmatrix} v_h\beta/\Omega \\ -r\sin(\beta+\psi) \\ -r\cos(\beta+\psi)+r-h \end{pmatrix}, \quad \vec{ds} = \frac{ds}{\sqrt{1+(\frac{v_h}{\Omega r})^2}} \begin{pmatrix} v_h/(\Omega r) \\ \cos(\beta+\psi) \\ -\sin(\beta+\psi) \end{pmatrix} \tag{5}$$

The induced velocity at the blade section s due to this vortex filament $\vec{ds}$ is calculated according to the Biot-Savart Law.

$$\vec{dw} = \frac{\Gamma}{4\pi}\frac{\vec{x}\times\vec{ds}}{|\vec{x}|^3} \tag{6}$$

According to Pirrung [3], the local inflow angle determined by local axial velocity v_h and rotational speed Ωr, is used as the helix angle φ, since the trailed vorticity close to the blade is supposed to be modelled.

$$\varphi = \tan^{-1}(v_h/\Omega r) \tag{7}$$

The axial induction, which is the x-component of $\vec{dw}$ is then as follows.

$$\begin{aligned} dw_x &= \frac{\Delta\Gamma}{4\pi}\frac{x_y ds_z - x_z ds_y}{|\vec{x}|^3} \\ &= \frac{\Delta\Gamma ds\cos\varphi}{4\pi r^2}\frac{1-(1-\frac{h}{r})\cos(\beta+\psi)}{\left[1+(1-\frac{h}{r})^2-2(1-\frac{h}{r})\cos(\beta+\psi)+(\beta\tan\varphi)^2\right]^{3/2}} \end{aligned} \tag{8}$$

The definition of the trailing function is different from that for the straight blade [5]. The new definition is the induced velocity normalized with dw_0^{st}, which is the induction of the corresponding straight blade ($\psi = 0$) at the starting point ($\beta = 0$).

$$\frac{dw_x}{dw_{0,x}^{st}} = \frac{(\frac{h}{r})^2\left[1-(1-\frac{h}{r})\cos(\beta+\psi)\right]}{\left[1+(1-\frac{h}{r})^2-2(1-\frac{h}{r})\cos(\beta+\psi)+(\beta\tan\varphi)^2\right]^{3/2}} \tag{9}$$

The tangential induction function is the normalized y-component of $\vec{dw}$ and is as follows.

$$\frac{dw_y}{dw_{0,y}^{st}} = \frac{(\frac{h}{r})^2\left[1-\frac{h}{r}-\cos(\beta+\psi)-\beta\sin(\beta+\psi)\right]}{\left[1+(1-\frac{h}{r})^2-2(1-\frac{h}{r})\cos(\beta+\psi)+(\beta\tan\varphi)^2\right]^{3/2}} \tag{10}$$

The derived equations are in similar form as the equations for the helical trailed wake derived by Pirrung [3]. For the special case of a straight blade which corresponds to $\psi = 0$, the equations derived above are identical to that derived in [3]. For the special case that the trailing vorticity stays in the rotor plane ($\varphi = 0$), the only difference between the trailing functions of the straight blade and the swept blade is that the variable of β is changed to $\beta+\psi$. This could be considered as simply applying a lead or lag in phase with the value of ψ. However, when the trailed vorticities are convected downstream ($\varphi > 0$), the blade sweep could not be simply considered as only adding phase difference to the trailing function.

3.1.2. Exponential approximation In order to use the indicial function algorithm for the fast calculation of NWM, the new exponential functions which approximate the analytical trailing function of the swept blade should be obtained.

One method is scaling the original trailing function of the straight blade in order to match the steady-state result of the analytical solution (the integral of the trailing function from 0 to $\pi/2$). This is similar to the root correction introduced by Pirrung [3]. This scaled original trailing function is compared with the analytical result in Figure 3.

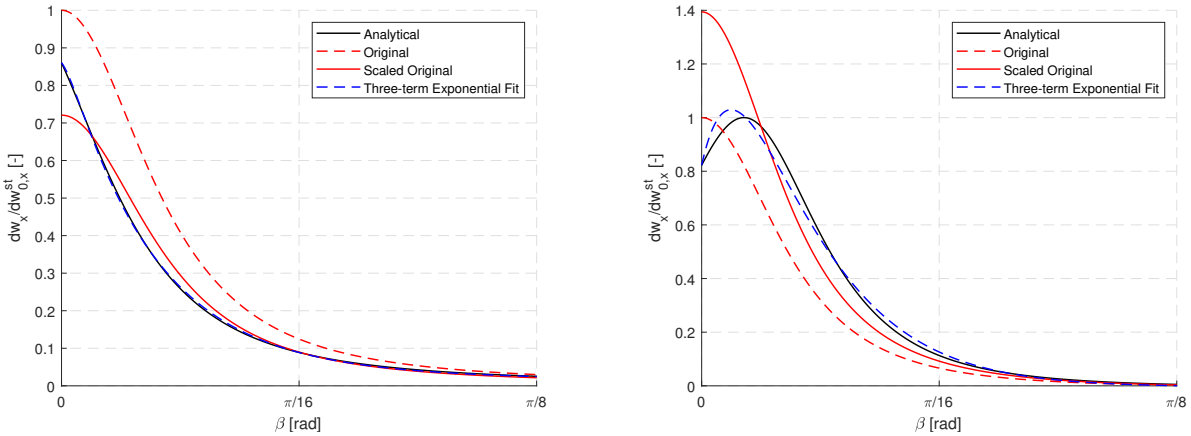

Figure 3. Comparison of the in-plane trailing functions for a backwards swept blade if the section point is inboard(left) with $h/r = 0.1$, $\psi = 2°$ and outboard(right) with $h/r = -0.1$, $\psi = -2°$.

As seen in Figure 3, the original model is not able to properly approximate the analytical trailing function which represents the dynamics of the induction due to trailing vorticity. Especially when the vorticity is trailed ahead of the blade section ($\psi < 0$), with the increase of β, the analytical trailing function firstly increase and then decrease. This is because the trailed vorticity element $\vec{ds}$ will firstly move closer to the section point and then move further away. This shape of the trailing function is not able to be modelled by the scaled original approximation based on two exponential functions. It is also shown in Figure 3 that it is possible to obtain a better approximation using a three-term exponential fit. The computational effort of the new method will increase less than 50% compared to the original one, and will still ensure fast calculation.

However, comparing to the straight blade, there is one additional variable ψ which describes the blade sweep geometry. So, the process of obtaining the new exponential functions will be more complex and lengthy than that for the straight blade in [4]. Due to the limitation of page length of this paper, only steady-state results calculated from analytical trailing functions will be presented in the following. The details about the new approximation of trailing function with three-term exponential functions and the corresponding dynamic response will be presented in the near future.

3.2. Bound Vorticity

The quarter chord points of the blade were implicitly assumed to form a straight lifting line in previous implementations of the NWM [1, 3, 5]. However, for the swept blade, the quarter chord points will follow the blade sweep and form a curved line as shown in Figure 2. This curved lifting line will then introduce additional induced velocity at the section points apart from the trailing vorticity.

However, when evaluating the induced velocity of the curved lifting line on itself according to the Biot-Savart Law, there will be singularity problems. Even though vortex core [11] could be introduced to eliminate singularities, the results will then be dependent on the vortex core size as well as discretization of the blade.

Alternatively, the induced velocities due to the lifting line, located at the quarter-chord points, is evaluated at the three-quarter chord points. For both straight blade and swept blade, the bound vorticity will induce velocity at the three-quarter chord points, which are noted as $W^{b,str}_{3/4\,c}$ and $W^{b,cur}_{3/4\,c}$ respectively. The additional induced velocity due to the curved lifting line, ΔW^b, is then approximated with Equation 11.

$$\Delta W^b \approx W^{b,cur}_{3/4\,c} - W^{b,str}_{3/4\,c} \tag{11}$$

where $W^{b,cur}_{3/4\,c}$ is calculated with the unsteady bound vorticity strength using the Biot-Savart Law, and $W^{b,str}_{3/4\,c}$ is calculated from the corresponding 'virtual' straight blade with the same vorticity distribution as the swept blade. The geometry of the 'virtual' straight blade is obtained from the swept blade by aligning the quarter chord points into a straight line while keeping their radius. To be noted that the three-quarter chord points are assumed to be in the rotor plane (neglect twist angle) since the lifting line is also assumed to be in-plane. Thus, ΔW^b will only influence the axial induction.

4. Results

There are five different wind turbine blades used for the validation of the modified NWM, all of them are based on the IEA 10MW RWT. The baseline straight blade is modified by aligning the quarter chord points to a straight main axis (except near the root where the centre of cylinder is aligned). For the backwards swept blades, the planforms are obtained from Bézier curves which are parameterized with: sweep ratio $\bar{r_s}$, sweep magnitude Δd and tip sweep angle Λ_{tip}. A sketch is shown in Figure 4 for demonstration, and the parameters of the four swept blades are summarized in Table 1. The cross-sections are rotated accordingly, so that the airfoils are perpendicular to the curved main axis. The chord and twist distribution of the blade remain the same as baseline blade. For a clean comparison, the pre-bend as well as cone angle of all blades are set to zero since the influence due to the vorticity starts trailing from out of the rotor plane is not modelled in the current NWM.

Table 1. The parameters of the planforms of four backwards swept blades

Name	Sweep ratio $\bar{r_s}$	Sweep magnitude Δd	Tip sweep angle Λ_{tip}
Blade 1	50%	10%	20°
Blade 2	50%	10%	40°
Blade 3	25%	5%	20°
Blade 4	25%	5%	40°

As introduced previously in Section 3, the influence of blade sweep on induced velocity is consisted of two parts which are the trailed vorticity and the curved lifting line. For the original NWM, straight lifting line is assumed, thus neither of the two effects are modelled. In order to evaluate the contribution of the two parts, two modified NWMs are introduced. The first

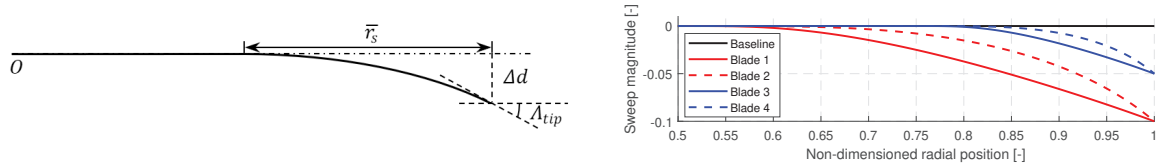

Figure 4. The parameterization of the swept blade (left) and the demonstration of the main axis of the swept blade as well as the baseline straight blade (right).

modified NWM only takes into account the influence due to trailed vorticity, and the second models the influence due to both trailed vorticity and bound vorticity. The two modified NWMs are noted as 'NWM Mod Trail' and 'NWM Mod Trail+Bound' respectively.

The surface meshes used in the CFD calculations were generated using an in-house meshing tool, and the volume meshes were generated using HypGrid3D [12], with 256 cells in chord-wise direction, 128 cells in both span-wise and normal direction with a first cell height of 1×10^{-6}m. In total, there were 14.16 million mesh cells in the volume mesh. The CFD results are calculated with the structured grid Reynolds-averaged Navier-Stokes (RANS) solver EllipSys3D [7] using a steady-state moving mesh approach [13], assuming fully turbulent flow in the wall surface boundary layer, using the $k-\omega-$SST turbulence model by Menter [14].

The BEM implemented in the HAWC2 [6] with tip loss correction is also used for the comparison. The blade sweep is modelled by using only the component of relative velocity which is projected in the airfoil cross-section for the calculation, and neglecting the span-wise component.

The normal and tangential forces, in normal operational condition with 8 m/s free wind speed and tip speed ratio of 10.58, are calculated for all blades with the aforementioned aerodynamic models. The normal and tangential forces are used for the following investigations and validations.

4.1. Straight blade

Firstly, the steady-state results of the baseline straight blade calculated from BEM, NWM and CFD are compared in Figure 5. The results from two modified NWMs are identical to that from the original NWM because the lifting line is straight.

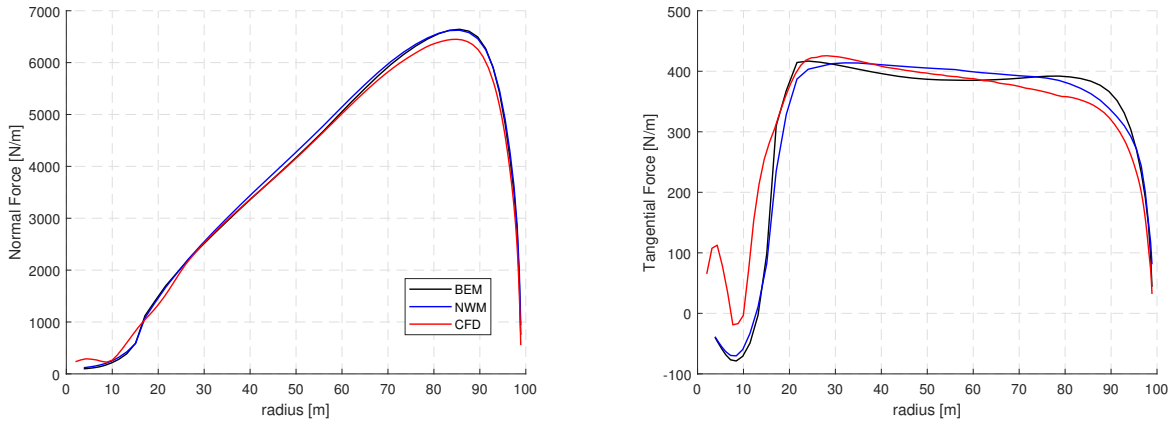

Figure 5. Comparison of normal and tangential forces of baseline straight blade calculated from BEM, NWM and CFD.

Despite the BEM and NWM are having some overestimation of both normal and tangential forces near the tip, the results are in good agreement with CFD results. The main reason is that both BEM and NWM utilize 2D airfoil polar data for the calculation of lift and drag coefficients (despite based on fully turbulent 2D CFD results), which will then be different from 3D CFD calculations. This is consistent with the conclusion obtained in [3].

4.2. Influence of bound and trail vorticity on swept blade

For the backwards swept blade, the load distributions from original NWM as well as the two modified NWMs are compared in Figure 6 for the swept Blade 3. Please note that the coupling factor calculated from the original NWM is applied to the two modified NWMs. This is because the influence of blade sweep is mainly from the near wake part (due to bound vorticity and trailed vorticity), which is not included in BEM. By using the same coupling factor from the original model, the far wake contribution will then be almost identical. For the modified NWM which takes into account influence due to both trail and bound vorticity, the normal force is flattened near the tip, and the tangential force near radius 80m is having a sudden decrease. These two effects are not able to be correctly modelled if the bound vorticity is not modelled. If only the trailed vorticity effect is included, the tangential force (and thus the power production) will increase on the whole swept parts of the blade relative to straight blade. It is the addition of the curved bound vorticity effect that brings the total tangential force down again, such that there are regions with both lower and higher production with respect to the baseline straight blade. All NWM computations presented in Section 4.3 include both the modified trailed and bound vorticity contributions.

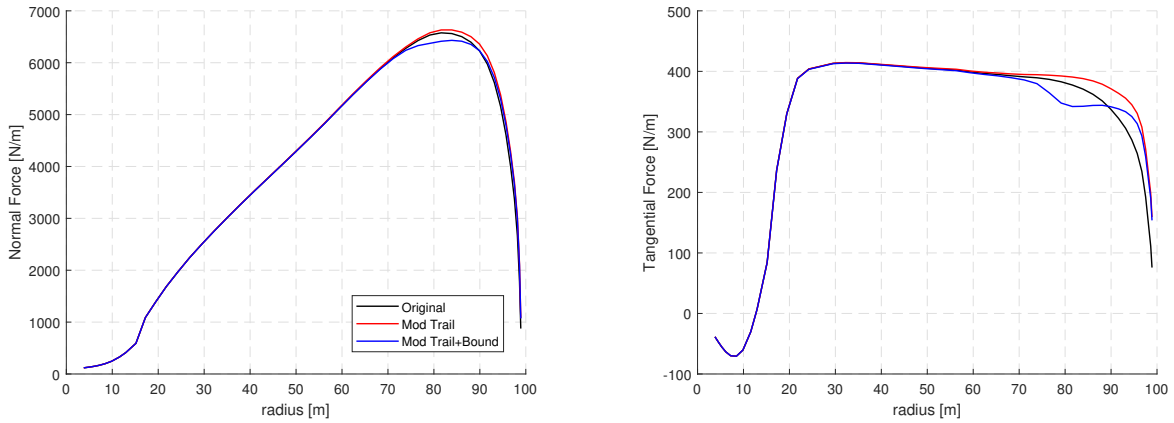

Figure 6. Comparison of the normal and tangential forces of Blade 3 calculated from original and modified NWMs.

4.3. Validation against CFD

Then, the steady-state results of the swept blades calculated from different aerodynamics models are validated against the CFD results. The normal and tangential forces of two swept blades with 20° of sweep as well as baseline straight blade calculated from modified NWM and CFD results are compared in Figure 7. The tangential load distribution of the swept blades from the modified NWM is in very good agreement with CFD results. Thus, it again indicates both the influences of bound and trailed vorticity due to blade sweep should be modelled. However, the normal force of Blade 1 seems to deviate from CFD results.

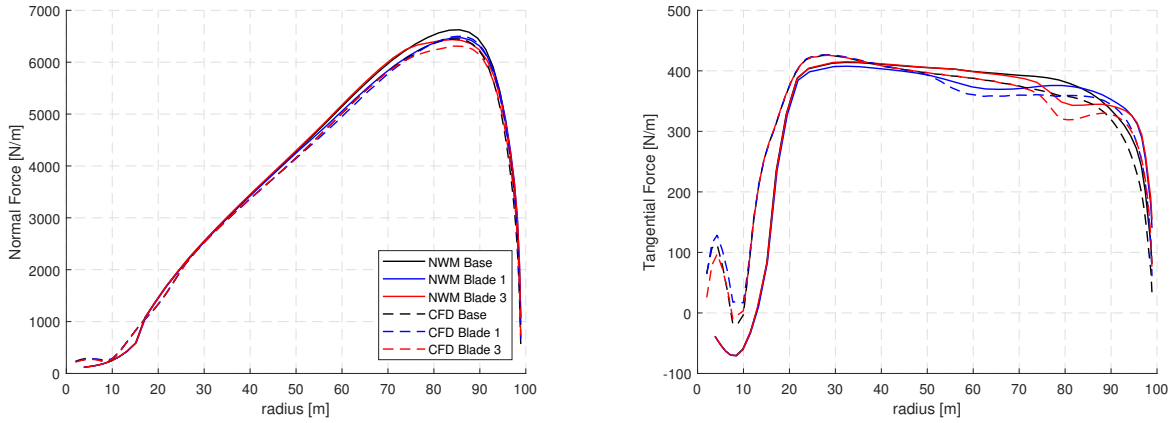

Figure 7. Comparison of the normal and tangential forces of the Blade 1 and Blade 3 with respect to the baseline straight blade calculated from modified NWM and CFD results.

In order to clearly show the influence of the backwards sweep on load distribution, the offset of the forces of the swept blade with respect to the baseline blade calculated from NWM as well BEM are compared against CFD results in Figure 8. It can be seen that for the swept blade, both the normal and tangential forces will be almost identical to the baseline blade where the blade is not swept. This justifies using the same coupling factor for the modified NWM and original NWM in Section 4.2. When moving outboard, both the normal and tangential forces are decreased compared to the baseline. This is approximately from where the backwards sweep begins until halfway to the tip. When moving further towards the tip, both normal and tangential forces are then increased compare to the baseline and until the blade tip. For the tangential forces, the aforementioned decrease and then increase of the offset could be very well modelled by the modified NWM, while the BEM predicts almost no difference between straight and swept blades. However, for the normal forces, the offsets calculated from BEM and modified NWM are both different than the CFD results.

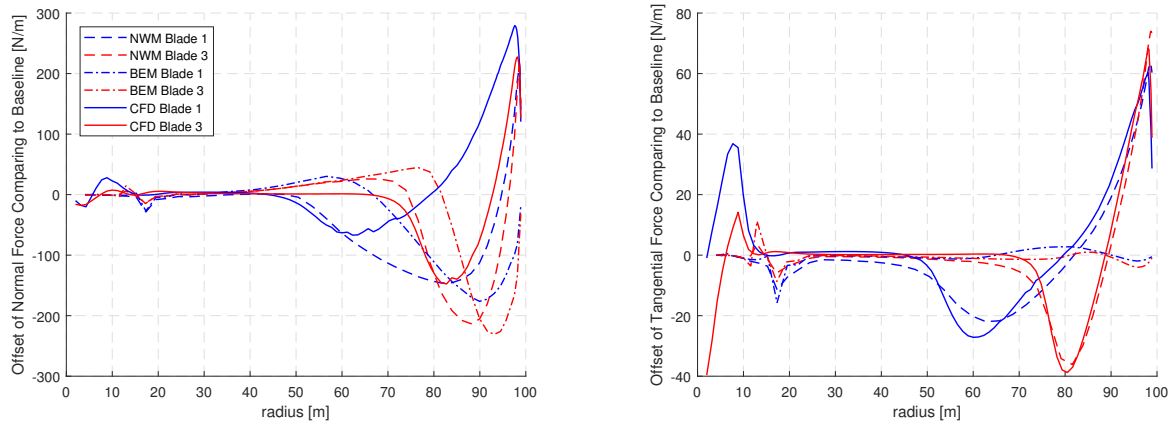

Figure 8. Comparison of the offset of normal and tangential forces of the Blade 1 and Blade 3 with respect to the baseline straight blade calculated from modified NWM and CFD results.

The NWM model is coupled with the BEM through a coupling factor and BEM is used to model the far wake. So, if the BEM could not correctly model the influence of blade sweep on

the normal load distribution, the error will then be inherited to the coupled near wake model. The modification proposed in this paper is intended to model the blade sweep by modifying the near wake part. Thus, in order to validate whether this modification is performed sufficiently, the error due to the BEM is subtracted. For all four swept blades, the normal force offset from the modified NWM minus that from BEM which is multiplied by the coupling factor and then compared with the CFD results in Figure 9.

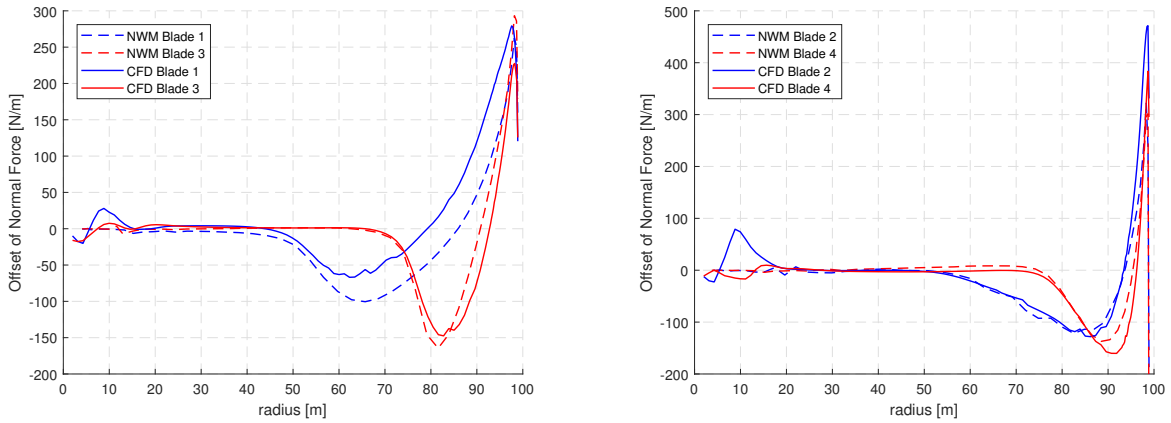

Figure 9. Comparison of the offset of normal force from modified NWM subtracting the offsets from BEM with CFD results for all four swept blades.

It can be seen that if the load difference due to sweep in the far wake BEM is subtracted, the offset of the normal force is now well predicted by the modified NWM for all four swept blades. Thus, in order to correctly model the normal forces of swept blades with NWM, further modifications should be made to the far wake BEM and maybe the coupling method as well.

5. Conclusion

The near wake model has been extended to compute the induction due to the trailed vorticity as well as the curved bound vorticity of the swept blade. The validation with full rotor CFD showed the influence due to blade sweep on the load distribution could be well modelled by the modified NWM with both the influence due to trailed vorticity of the swept blade and due to the curved lifting line modelled. If the influence of the curved bound vorticity is neglected, wrong results and conclusions will be obtained. For the original NWM as well as the BEM, neither of the aforementioned two effects due to blade sweep is correctly modelled, the results are having large differences compared to the CFD results. For the normal force, it was shown that since the BEM is not able to correctly model the influence due to blade sweep, the error is inherited to the NWM models through the far wake BEM. However, if the error due to BEM is subtracted from NWM results, the modified NWM is able to correctly predict the influence on normal forces.

In conclusion, the proposed modification to the near wake model in this work is able to correctly model the influence due to the blade sweep. However, in order to model the steady-state normal forces of swept blades correctly, future work should be done to the far wake BEM which is coupled with NWM. In addition, future work should be done to obtain the three-term functions, which approximate the analytical trailing functions, in order to model the dynamic response of the swept blades with a higher accuracy.

Acknowledgement
The work has been conducted within the project "SmartTip" which is funded by "Innovation Fund Denmark".

References

[1] T. S. Beddoes. A near wake dynamic model. In *Aerodynamics and Aeroacoustics National Specialist Meeting. Papers and Discussion*, pages 1–9, 1987.
[2] H. Aa. Madsen and F. Rasmussen. A near wake model for trailing vorticity compared with the blade element momentum theory. *Wind Energy*, 7(4):325–341, 2004.
[3] G. R. Pirrung, H. Aa. Madsen, T. Kim, and J. Heinz. A coupled near and far wake model for wind turbine aerodynamics. *Wind Energy*, 19(11):2053–2069, 2016.
[4] G. R. Pirrung, H. Aa. Madsen, and S. Schreck. Trailed vorticity modeling for aeroelastic wind turbine simulations in standstill. *Wind Energy Science*, 2(2):521–532, 2017.
[5] G. R. Pirrung, M. H. Hansen, and H. Aa. Madsen. Improvement of a near wake model for trailing vorticity. In *Journal of Physics: Conference Series*, volume 555, page 012083. IOP Publishing, 2014.
[6] T. Juul Larsen, A. Melchior Hansen, and Wind Energy Dept. Risø National Lab., DTU. *How 2 HAWC2, the user's manual*. 2007.
[7] Niels N. Sørensen. *General purpose flow solver applied to flow over hills*. PhD thesis, 1995. Published 2003.
[8] F. Zahle, K. Dykes, P. E. Rethore, and K. Merz. IEA-10.0-198-RWT. https://github.com/IEAWindTask37/IEA-10.0-198-RWT. Online; Accessed: 2018-03-09.
[9] G. R. Pirrung, V. Riziotis, H. Aa. Madsen, M. H. Hansen, and T. Kim. Comparison of a coupled near- and far-wake model with a free-wake vortex code. *Wind Energy Science*, 2(1):15–33, 2017.
[10] T. Wang and F. N. Coton. A high resolution tower shadow model for downwind wind turbines. *Journal of Wind Engineering and Industrial Aerodynamics*, 89(10):873–892, 2001.
[11] J. Katz and A. Plotkin. *Low-speed aerodynamics*, volume 13. Cambridge University Press, 2001.
[12] Niels N. Sørensen. HypGrid2D—a 2-D mesh generator. Technical report, Risø-R-1035(EN), Risø National Laboratory, 1998.
[13] Niels N. Sørensen. Rotor computations using a 'steady state' moving mesh. IEA Joint Action Committee on aerodynamics. Annex XI and 20. Aero experts meeting, Pamplona (ES), 25-26 May 2005.
[14] F. R. Menter. Zonal two-equation $k-\omega$ models for aerodynamic flows. *AIAA paper 93-2906*, 1993.